XL CILAMCE
IBERO-LATIN AMERICAN CONGRESS ON COMPUTATIONAL METHODS IN ENGINEERING
NOVEMBER 11-14, 2019
Praiamar Natal Hotel & Convention Natal, RN-BRAZIL

VIBRATION CONTROL USING THE STRUCTURAL COUPLING TECHNIQUE BETWEEN ADJACENT BUILDINGS WITH DIFFERENT CONTROL DEVICES

Augusto S. Pippi
augustopippi@hotmail.com
Postgraduate Program in Structures and Civil Construction
University of Brasilia, Campus Darcy Ribeiro, 70910-900, Brasilia, Federal District, Brazil
Suzana M. Avila
avilas@unb.br
Postgraduate program in Engineering Materials Integrity
University of Brasilia, College of Gama, 72444-420, Brasilia, Federal District, Brazil
André M. de Almeida
andremurilo@unb.com
Postgraduate Program in Mechatronics Systems
University of Brasilia, College of Gama, 72444-420, Brasilia, Federal District, Brazil
Graciela Doz
graciela@unb.br
Postgraduate Program in Structures and Civil Construction
University of Brasilia, Campus Darcy Ribeiro, 70910-900, Brasilia, Federal District, Brazil

Abstract. The use of structural control in vibration mitigation is becoming increasingly common in buildings. Forces of nature such as wind and earthquakes show how buildings are vulnerable to their actions. A control technique that is gaining space is the structural coupling. This technique consists of connecting two adjacent structures using different control devices, so that control forces are exerted from one structure on the other to reduce the dynamic response of each structure individually and the coupled system. To study the efficiency of this technique, a system containing two adjacent structures was used. The system was modeled as having two degrees of freedom and subjected to seismic action of three earthquakes with different frequencies. In the first step of the analysis, a passive control device was used. The device parameters were optimized through a particle swarm optimization algorithm. In the second step, an actuator was used, an active control device, in which it was optimized by the Linear Quadratic Regulator. Finally, in the last step, the two devices, passive and active, were used together, composing an hybrid control. The results indicated the importance of the structure response in the performance of each control device. The coupling technique proved effective in mitigating vibration amplitude, with reductions of up to 80% in displacements and 85% in velocities and accelerations.

Keywords: Structural control, Structural coupling, LQR Controller, Passive control, Hybrid control

1 Introduction

Excessive vibration in buildings is an increasingly evident problem. With a higher population density in urban centers, buildings grow vertically and, due to their higher heights, there is greater slenderness in these structures. Also, 1940 El Centro, 1994 Northridge and 1995 Kobe earthquakes, demonstrated the vulnerability of building construction to dynamic actions.

In order to control excessive vibrations, structural control techniques are used. In addition to increasing the reliability level, these techniques generate material savings and allow the construction of structures with a low level of vibrations. Commonly, control types are classified into: passive, active, semi-active and hybrid. Essentially, vibration control devices act to absorb energy from the structure, reducing the amplitude of vibrations [1-4].

Active control devices apply forces to the structure through actuators that are connected to an external power source. This type of control requires algorithms that work through the response of the structure measured by sensors and calculate in real time the magnitude of these forces [5-6]. The basic form of an active controller is shown in Fig. 1. Passive control devices do not require an external power source. They are widely used in vibration control as they do not require the use of high technology. In addition, they have been used for a long time and their reliability and efficiency has been proven [6-8]. When two or more control types are combined, the technique is called hybrid control. Normally hybrid control systems require forces of smaller magnitudes on the actuators. In addition, they operate at a wider frequency range compared to passive control [6].

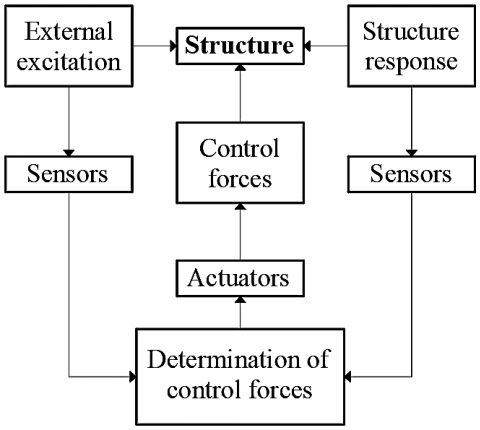

Figure 1. Schematic of an active type controller

Another control technique that has been shown to be effective in mitigating vibrations is structural coupling. The principle of this technique is to connect two adjacent structures by connecting elements using different control devices. Thus, control forces are exerted from one structure to another to reduce the dynamic response of each structure individually and the coupled system [10-18]. Initially suggested by Klein *et al.* [9], structural coupling has been increasingly studied for its good performance in controlling excessive vibration and preventing pounding between nearby buildings.

Due to the advantages of the hybrid control and the efficiency of the structural coupling technique, the aim of this work is to verify the performance of the combined use of the two control techniques in an adjacent spring mass damper of two degree of freedom system. The passive control device has its mechanical properties, damping and stiffness, optimized through the particle swarm optimization (PSO) algorithm. In active control, an actuator controlled by the Linear Quadratic Regulator (LQR) algorithm will be used.

2 Coupling of adjacent structures

Structural coupling to adjacent structures is a type of structural control used to attenuate the amplitude of vibrations in structures subject to earthquake and high wind action. Studies performed by

Klein *et al.* [9] suggested a simple coupling, connecting two structures with cables capable of stretching and shortening to provide control forces. Already in 1987, Klein and Healy [22] proposed an algorithm for semi-active control, in which two adjacent buildings were connected by cables. In their studies, the authors found that to ensure system controllability it was necessary that the main natural frequencies of buildings should be distinct. These studies were the precursors for several published works on the subject [10-19, 23-31].

Graham's studies [10] indicated that the use of active controllers in connecting adjacent structures is more effective when compared to passive control. This is due to their adaptability to different load conditions. Christenson [23] used active control to mitigate vibrations from experimentally coupled adjacent structures. It was seen that accelerations were significantly reduced, indicating the effectiveness of active control. Also, there was a reduction in the coupled system response time.

Using the LQR optimization algorithm, Christenson *et al.* [15] and Zhu *et al.* [24] conducted a comparative study of the use of different coupling devices in adjacent structures. In both studies, the use of semi-active [24] and active [15] dampers were more effective in the performance of decreasing vibration amplitude when compared to a passive control device. Pérez *et al.* [27] found in their studies that the effectiveness of the control method depends mainly on the properties of mass, stiffness and damping of adjacent structures.

Palacios-Quinõnero *et al.* [28] proposed a control strategy by connecting two adjacent buildings with a passive actuator along with an active actuator on each floor. They found that when the active control system fails, a considerable reduction in the maximum inter-story drifts in both buildings is achieved by passive control. Pérez *et al.* [16] connect two adjacent buildings with a passive control device along with an active control device. It was found that the passive control system has no negative effect on the performance of the active control system. Studies by Park and Ok [29] showed that the use of the coupling technique in two adjacent structures with similar natural frequencies connected with a hybrid control device is efficient in vibration control.

2.1 Mathematical modeling for coupled systems with 2 degrees of freedom (2DOF)

In Fig. 2 it is illustrated an equivalent system of two adjacent coupled structures with fixed-base. The formulation is based on the work of [6, 10, 27].

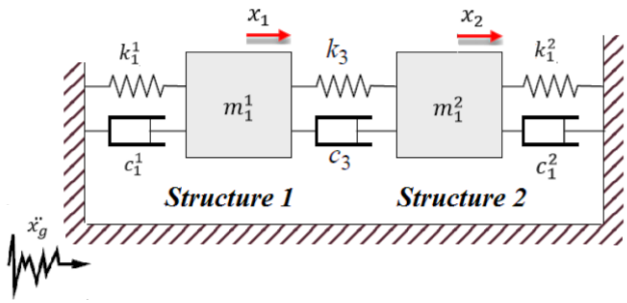

Figure 2. System of coupled adjacent structures

In the figure above m_1^1 and m_1^2 are the masses, k_1^1 and k_1^2 the stiffness and c_1^1 and c_1^2 the damping of the structures 1 and 2, respectively. Moreover, k_3 and c_3 are the stiffness and damping coefficient, respectively, of the connection between the two structures and $\ddot{x}_g$ an acceleration at the base of the system. The equations of motion for the two degree of freedom system is given by Eq. (1), where, $\boldsymbol{M}$, $\boldsymbol{C}$ and $\boldsymbol{K}$ are, respectively, the mass, damping and stiffness matrices of the coupled system; $\boldsymbol{x}(\boldsymbol{t})$ is the system displacement vector.

$$\boldsymbol{M}\ddot{\boldsymbol{x}}(\boldsymbol{t}) + \boldsymbol{C}\dot{\boldsymbol{x}}(\boldsymbol{t}) + \boldsymbol{K}\boldsymbol{x}(\boldsymbol{t}) = -G\ddot{x}_g \tag{1}$$

$$\boldsymbol{M} = \begin{bmatrix} m_1^1 & 0 \\ 0 & m_1^2 \end{bmatrix}, \quad \boldsymbol{C} = \begin{bmatrix} c_1^1 + c_3 & -c_3 \\ -c_3 & c_1^2 + c_3 \end{bmatrix}, \quad \boldsymbol{K} = \begin{bmatrix} k_1^1 + k_3 & -k_3 \\ -k_3 & k_1^2 + \mathrm{k}_3 \end{bmatrix}, \quad G = \boldsymbol{M}\begin{Bmatrix} 1 \\ 1 \end{Bmatrix} \tag{2}$$

2.2 State space representation of coupled buildings

The state space representation for the two degree of freedom coupled system is given by:

$$\dot{\boldsymbol{z}}(t) = \boldsymbol{A}\boldsymbol{z}(t) + \boldsymbol{B_f}F + \boldsymbol{B_u}u \tag{3}$$

Where, $\boldsymbol{z}(t)$ is the state vector, $\boldsymbol{A}$ is the system state matrix, $\boldsymbol{B_f}$ is the disturbance matrix, $\boldsymbol{B_u}$ is a location matrix, F is the system input excitation and u is the control forces.

$$\boldsymbol{z}(t) = \begin{bmatrix} z_1 \\ z_2 \\ z_3 \\ z_4 \end{bmatrix} = \begin{bmatrix} x_1 \\ x_2 \\ \dot{x}_1 \\ \dot{x}_2 \end{bmatrix} \tag{4}$$

$$\boldsymbol{A} = \begin{bmatrix} 0 & 0 & 1 & 0 \\ 0 & 0 & 0 & 1 \\ -\frac{k_1^1+k_3}{m_1^1} & \frac{k_3}{m_1^1} & -\frac{c_1^1+c_3}{m_1^1} & \frac{c_3}{m_1^1} \\ \frac{k_3}{m_1^2} & -\frac{k_1^2+k_3}{m_1^2} & \frac{c_3}{m_1^2} & -\frac{c_1^2+c_3}{m_1^2} \end{bmatrix}, \quad \boldsymbol{B_f} = \begin{bmatrix} 0 & 0 \\ 0 & 0 \\ 1 & 0 \\ 0 & 1 \end{bmatrix}, \quad \boldsymbol{B_u} = \begin{bmatrix} 0 & 0 \\ 0 & 0 \\ 1 & 0 \\ 0 & 1 \end{bmatrix} \tag{5}$$

The output equation is defined as:

$$\boldsymbol{y}(t) = \boldsymbol{C}\boldsymbol{z}(t) \tag{6}$$

Where, $\boldsymbol{y}(t)$ is the output vector and $\boldsymbol{C}$ the output matrix. For this case, the matrix $\boldsymbol{C}$ is an identity matrix with 4x4 dimension.

3 LQR controller

One of the main elements in the use of structural control techniques is an effective control algorithm to compute the magnitude of the internal forces to be applied to the structure [20-21]. The Linear Quadratic Regulator is one of the most widely used techniques for vibration control in structures subject to seismic actions. It is mainly used for active and semi-active type controls [20-21, 32-37]. LQR offers a systematic way of calculating the feedback gain matrix of each state and produces a stable system at the end. Optimal control forces are determined by minimizing the following cost function:

$$J = \int_{t_0}^{t_f} [\boldsymbol{z^T}(t)\boldsymbol{Q}\boldsymbol{z}(t) + \boldsymbol{u^T}(t)\boldsymbol{R}\boldsymbol{u}(t)]dt \tag{7}$$

where t_0 is the initial time and t_f is the finishing time of interest. The matrices $\boldsymbol{Q}$ and $\boldsymbol{R}$ are weighting matrices whose magnitudes depend on the importance of each state variable and the control forces in the minimization process. In addition, the matrix $\boldsymbol{Q}$ is chosen to be semi-definite positive ($\boldsymbol{Q} = \boldsymbol{Q^T} \geq 0$) and matrix $\boldsymbol{R}$ is positive symmetric ($\boldsymbol{R} = \boldsymbol{R^T} > 0$). The control forces are given by:

$$\boldsymbol{u}(t) = -\boldsymbol{G}\boldsymbol{z}(t) \tag{8}$$

Where $\boldsymbol{G}$ is the feedback gain matrix, and is given by:

$$\boldsymbol{G} = \boldsymbol{R^{-1}}\boldsymbol{B_u^T}\boldsymbol{P} \tag{9}$$

The matrix $\boldsymbol{P}$ is determined by the Ricatti algebraic equation:

$$\boldsymbol{P}\boldsymbol{A} - \boldsymbol{P}\boldsymbol{B_u}\boldsymbol{R^{-1}}\boldsymbol{B_u^T}\boldsymbol{P} + \boldsymbol{A^T}\boldsymbol{P} + \boldsymbol{Q} = \boldsymbol{0} \tag{10}$$

The controlled system is follow:

$$\dot{\boldsymbol{z}}(t) = (\boldsymbol{A} - \boldsymbol{B_u}\boldsymbol{G})\boldsymbol{z}(t) + \boldsymbol{B_f}F \tag{11}$$

Thus, the effect of closed loop control is the modification of the state matrix $\boldsymbol{A}$ (open loop system) for $\boldsymbol{A} - \boldsymbol{B_u}\boldsymbol{G}$ (closed loop system) [6]. In Fig. 3 a schematic of the closed loop control system is presented.

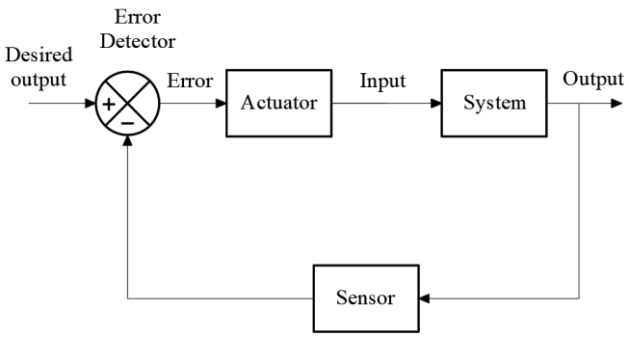

Figure 3. Closed-loop control scheme

4 Particle swarm optimization (PSO)

This algorithm was used to optimize the mechanical properties of the passive control device. The Particle Swarm Optimization algorithm (PSO) is based on a population of individuals who adapt and return stochastically to previously well-defined regions. It was developed by Kennedy and Eberhart [38] and is inspired on the behavior of fish, bees and other animals. It is an easy algorithm to implement and requires less calculation time to minimize when compared to other methods [39].

The total objective function used is presented in Eq. (14) and consists of two parts. The first, Eq. (12), is to minimize the square of the maximum displacement of the two adjacent buildings. The second, Eq. (13), aims to decrease the value of the sum of squares of these displacements.

$$f_{obj1} = \max\{(\{\Delta\}^1)^2 \quad (\{\Delta\}^2)^2\} \tag{12}$$

$$f_{obj2} = (\{\Delta\}^1)^2 + (\{\Delta\}^2)^2 \tag{13}$$

$$f_{objtotal} = f_{obj1} + f_{obj2} \tag{14}$$

where $\{\Delta\}^j$ is maximum displacement of each structure, being $(j = 1, 2)$.

5 Numerical analysis

Numerical analysis was performed using algorithms developed in MATLAB®. The system illustrated in Fig. 2 was subjected to the action of three different ground motions: 1940 El Centro, 1994 Northridge and 1995 Kobe earthquakes. The excitations are applied at the base and have dominant frequency ranges between 0.3 and 7.0 Hz. In this way, a good frequency range is considered to evaluate the behavior of the models.

In the first step, the algorithm using PSO was used to find the optimal values of damper constants k_3 and c_3 that connect the two masses. Thus, a passive type control is used. Stiffness ranges from zero to 6.10^6 N/m and zero damping up to 6.10^6 Ns/m, based on industry-available dampers (Taylor Device, Inc.).

In the second stage, the two masses are connected by an actuator, and the damper of the first stage is disregarded. Using a feedback system, the gain matrix $\boldsymbol{G}$ was calculated using the solution of Riccati equation, whose algorithm is used in MATLAB. Thus, it is possible to determine closed-loop system, according to Eq. (10), this control being active. Finally, both types of controls were used together to verify the efficiency of controlling the system. This type of control is called a hybrid one.

The mass, damping and stiffness values of each structure are reference values used by Pérez *et al.* [27] and are presented in Table 1.

Table 1. Properties of uncoupled structures [27]

Structure	Mass (kg)	Damping coefficient (Ns/m)	Stiffness coefficient (N/m)
1	30000	36860	1.2580E+07
2	82267	44986	6.8331E+06

For LQR optimization the $\boldsymbol{Q}$ and $\boldsymbol{R}$ weighting matrices were chosen based on Graham's work [10].

$$\boldsymbol{Q} = \begin{bmatrix} 1 & 0 & 0 & 0 \\ 0 & 1 & 0 & 0 \\ 0 & 0 & 1 & 0 \\ 0 & 0 & 0 & 1 \end{bmatrix}, \quad \boldsymbol{R} = \begin{bmatrix} 0.01 & 0 \\ 0 & 0.01 \end{bmatrix} \tag{15}$$

5.1 Results and discussions

The first stage optimization results for the three earthquakes are presented in Table 2.

Table 2. Optimization results

Earthquake	c_3	k_3	$f_{objtotal}$
El Centro	751190	0.00	0.004025
Northridge	222790	1.9838E+06	0.016184
Kobe	319670	2.9395E+06	0.025621

Due to the different frequency ranges of earthquakes considered, the determined constants are distinct. For the El Centro earthquake, the constant $k_3 = 0$ indicates a viscofluid damper, while for the Northridge and Kobe earthquakes they are viscoelastic dampers. A comparison between the displacements time history in structures 1 and 2 for the uncoupled, passive control, active control and hybrid control system is presented in Fig. 4 for the El Centro earthquake, in Fig. 5 for Northridge earthquake and Fig. 6 to Kobe earthquake. The velocities are shown in Fig. 7, Fig. 8 and Fig. 9, for El Centro, Northridge and Kobe earthquakes, respectively. In Fig. 10, Fig. 11 and Fig. 12 the accelerations are shown in the same way.

For passive control, in the El Centro earthquake there was a 65% increase in the maximum displacement of structure 1. However, for structure 2, there was a reduction of 49%. For Northridge earthquake there was a 50% of reduction in the maximum displacement of structure 1. In structure 2 this reduction was 43%. In the Kobe earthquake, structure 1 achieved an insignificant reduction. However, for structure 2, there was a 67% of reduction in the largest displacement.

Unlike passive control, efficiency was obtained in reducing the displacements in both structures for the three earthquakes considering active control. For El Centro earthquake there was a 52% of reduction in the displacement of structure 1. In structure 2, 73% of reduction in maximum displacement was achieved. For the Kobe earthquake, there was a 51% and 77% of reduction in the maximum displacement of structure 1 and structure 2, respectively. In the Northridge earthquake, the reductions in displacements were 62% in structure 1 and 66% in structure 2. These percentages are in agreement with the values obtained by Graham [10].

Hybrid control showed slightly lower efficiency than active control, but more efficient than passive control in reducing vibration amplitude.

By coupling the structures with a hybrid control system, there was a 20% reduction in the vibration amplitude of structure 1 for de El Centro earthquake. In structure 2, the reduction was 76%. In the Northridge earthquake, the reductions were on average 65%. In the structure 2, for the Kobe earthquake, the reduction in vibration amplitude reached 77%.

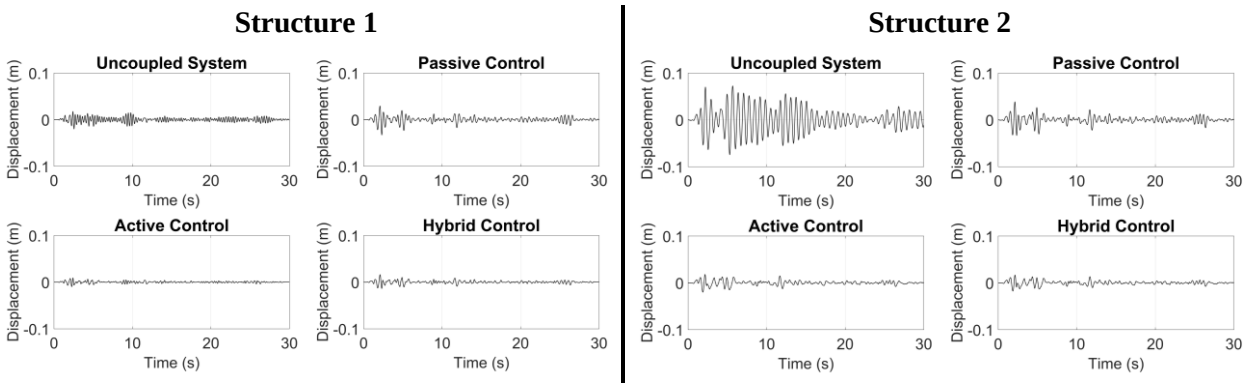

Figure 4. Displacement response for El Centro earthquake.

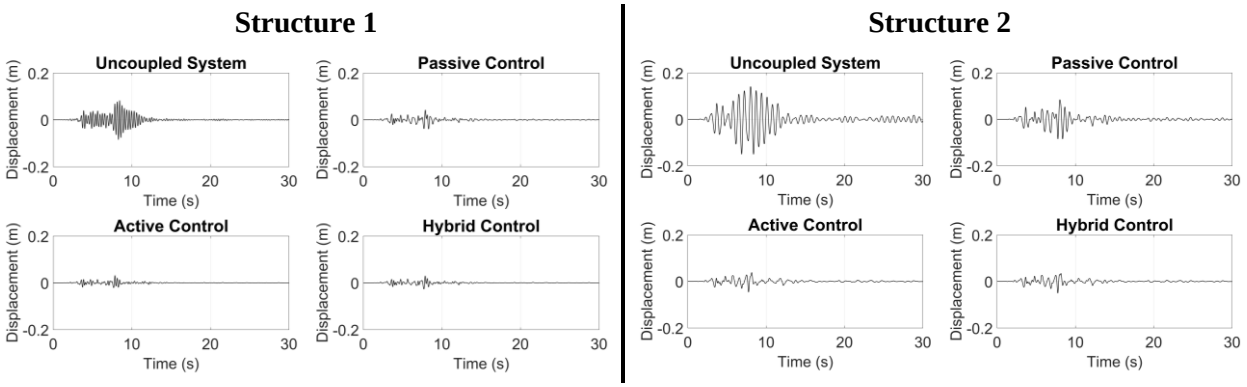

Figure 5. Displacement response for Northridge earthquake.

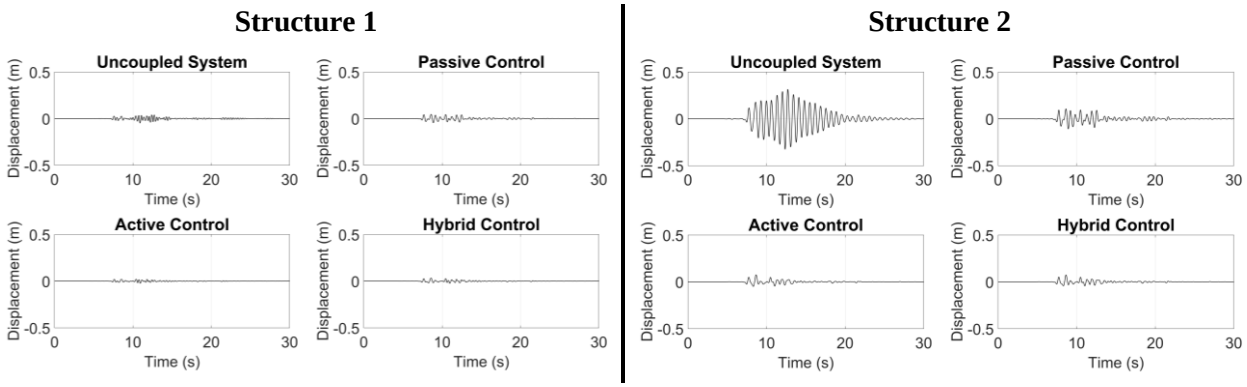

Figure 6. Displacement response for Kobe earthquake.

In the velocities, for passive control, there was a slight increase of 6% in structure 1 for the El Centro earthquake. In Northridge earthquake, there was a 54% of reduction in structure 1 and 18% of reduction in structure 2. For Kobe earthquake, in structure 1 velocities reduced by 22% and for structure 2 reduced by 60%.

Reductions of 70% were obtained in the active and hybrid control. In the Northridge and Kobe earthquakes, the efficiency of the active and hybrid controls are close, with reductions of up to 81% in maximum velocities.

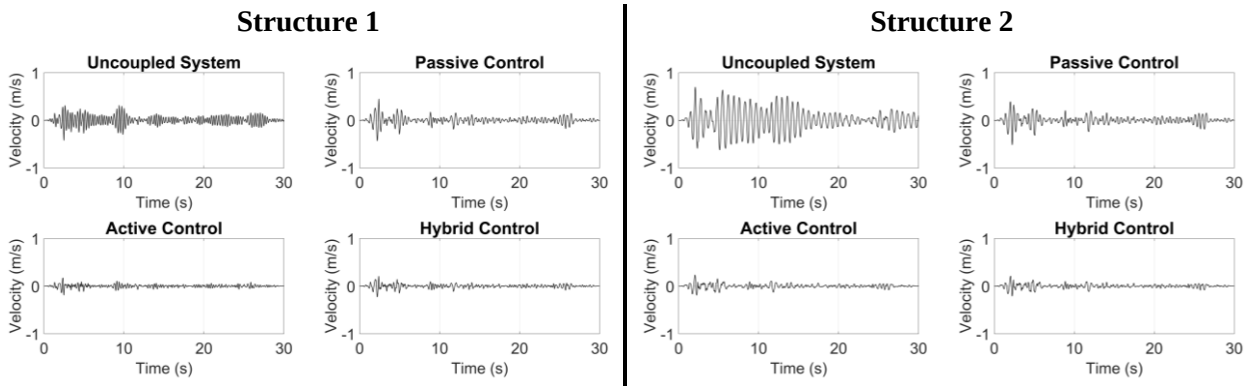

Figure 7. Velocity response for El Centro earthquake.

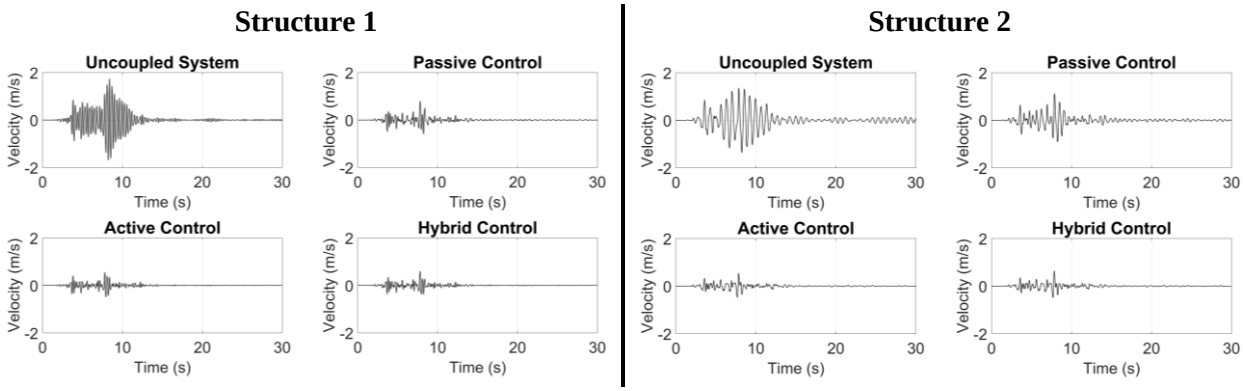

Figure 8. Velocity response for Northridge earthquake.

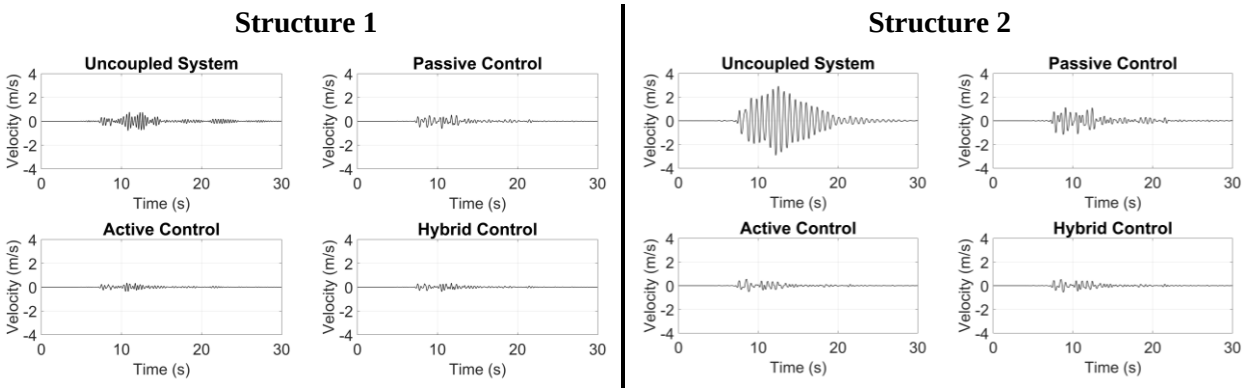

Figure 9. Velocity response for Kobe earthquake.

The same behavior of the displacement responses was obtained in the acceleration response. For the El Centro earthquake, there was a 66% increase in structure 1 acceleration when using the passive control system. Reductions in active control were 73% and in hybrid control 76% in structure 2. The largest reductions were obtained in the Kobe earthquake, reducing 77% in accelerations for active and hybrid control.

Table 3 shows the maximum displacement responses in structures 1 and 2 for the three earthquakes studied. Table 4 shows the maximum velocity results and table 5 the maximum acceleration results.

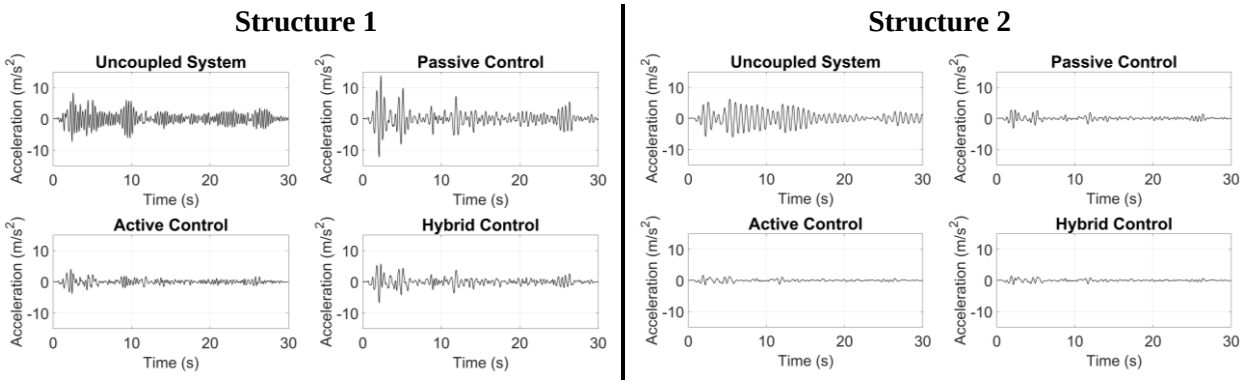

Figure 10. Acceleration response for El Centro earthquake.

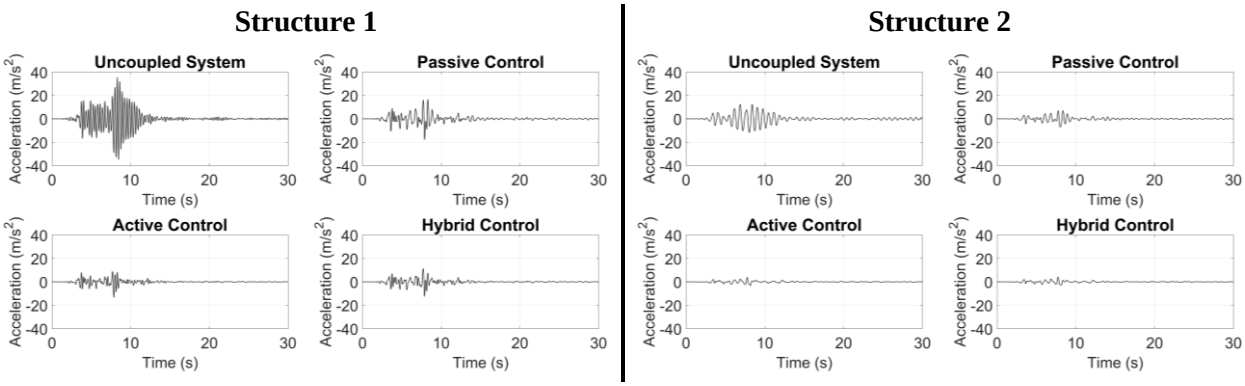

Figure 11. Acceleration response for Northridge earthquake.

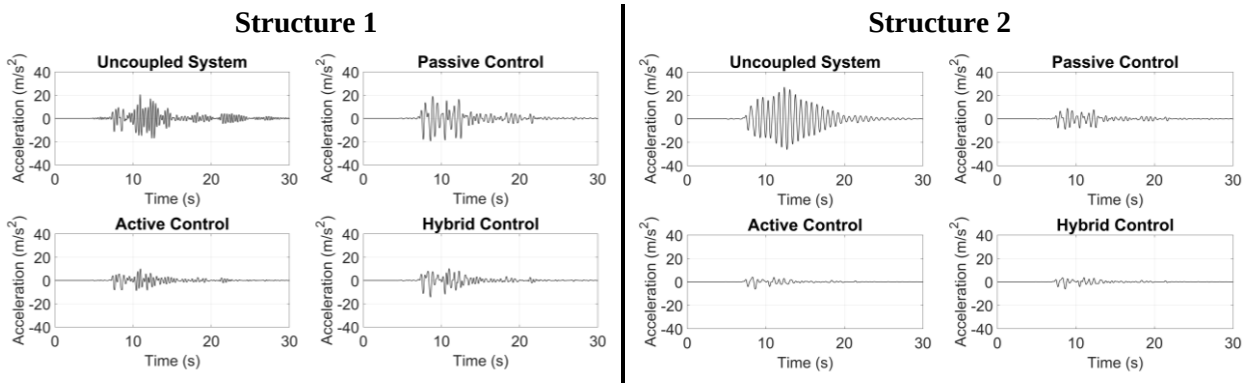

Figure 12. Acceleration response for Kobe earthquake.

Table 3. Maximum displacement response (m)

Earthquake	Structure	Control System			
		Uncoupled	Passive	Active	Hybrid
El Centro	1	0.020	0.033	0.010	0.016
	2	0.075	0.038	0.020	0.018
Northridge	1	0.085	0.042	0.032	0.030
	2	0.150	0.085	0.046	0.051
Kobe	1	0.049	0.047	0.024	0.034
	2	0.327	0.108	0.076	0.075

Table 4. Maximum velocity response (m/s)

Earthquake	Structure	Control System			
		Uncoupled	Passive	Active	Hybrid
El Centro	1	0.42	0.45	0.19	0.23
	2	0.70	0.51	0.23	0.21
Northridge	1	1.75	0.80	0.56	0.60
	2	1.37	1.13	0.55	0.64
Kobe	1	0.80	0.62	0.36	0.38
	2	2.94	1.16	0.56	0.55

Table 5. Maximum acceleration response (m/s^2)

Earthquake	Structure	Control System			
		Uncoupled	Passive	Active	Hybrid
El Centro	1	8.33	13.80	4.09	6.73
	2	6.21	3.22	1.66	1.46
Northridge	1	35.63	17.80	13.37	12.53
	2	12.51	7.06	3.86	4.23
Kobe	1	20.60	19.60	10.08	14.47
	2	27.16	9.06	6.31	6.22

6 Conclusions

A comparative study using different control devices in the structural coupling technique was performed in this work. Two adjacent structures with distinct dynamic characteristics were used. The structures were subjected to seismic action using the accelerations records of three different earthquakes. The devices compared are the passive control, optimized through the particle swarm algorithm, the active control using a linear quadratic regular and finally the hybrid control using the two techniques together.

In passive control, the optimization results suggest different dampers, which indicates the influence of the frequency range of the earthquakes used. In reducing the amplitude of vibrations, this type of control was effective in structure 1 only for the Northridge earthquake. However, for structure 2, this device was suitable for all three earthquakes.

The active control performance was satisfactory in all three earthquakes for structures 1 and 2. Velocity and acceleration reductions of 80 % were established. These results are in agreement with authors who also used active control in vibration mitigation [10, 15, 24].

Hybrid control proved to be more effective for the Northridge earthquake when compared to the separate use of each control device. It can be noted the dynamic characteristics along with the characteristics of earthquakes, influence the performance of each device. Importantly, active control devices require an external power source for their operation. This can become a major disadvantage in a seismic action. Depending on the purpose, choosing to use both devices together may be a solution to this difficulty, as active control has little effect on passive control performance.

Acknowledgements

The authors gratefully acknowledge the Brazilian agency CAPES (Council of National Scientific and Technological Development) for financial support of this research.

References

[1] G. W. Housner, L. A. Bergman, T. K. Caughey, *et al.* Control: Past, Present, and Future. *Journal of Engineering Mechanics*, vol. 123, n. 9, pp. 897-971, 1997.
[2] T. T. Soong and G. F. Dargush. *Passive energy dissipation systems in structural engineering*. John Wiley & Sons, 1997.
[3] T. T. Soong and B. F. Spencer Jr, 2000. Active, Semi-Active and Hybrid Control of Structures. *Proceedings of the 12th World Conference on Earthquake Engineering* (12WCEE), pp. 1-16.
[4] B. F. Spencer Jr. and S. Nagarajaiah. State of the Art of Structural Control. *Journal of Structural Engineering*, ASCE, vol. 129, n. 7, pp. 845-856, 2003.
[5] T. T. Soong. *Active structural control, theory & practice*. John Wiley & Sons, 1990.
[6] S. M. Avila. Controle Híbrido para Atenuação de Vibrações em Edifícios. Tese de doutorado, Pontifícia Universidade Católica do Rio de Janeiro, 2002.
[7] D. Jurukovski, M. Petkovski, Z. Rakicevic. Current Status of Building Passive Control in Japan. *Engineering Structures*, vol. 17, n. 5, pp. 319-333, 1995.
[8] T. T. Song, G. F. Dargush. *Passive energy dissipation systems in structural engineering*. John Wiley & Sons, 1997.
[9] R. E. Klein, C. Cusano and J. Stukel, 1972. Investigation of a method to stabilize wind induced oscillations in large structures. *ASME Winter Annual Meeting*, Paper n. 72.
[10] M. C. Graham. Design Strategies for Coupling Buildings. Master's Thesis, Massachusetts Institute of Technology, 1994.
[11] B. D. Westermo. The Dynamics of Interstructural Connection to Prevent Pounding. *Earthquake Engineering and Structural Dynamics*, vol. 18, pp. 687-699, 1989.
[12] J. E. Luco and C. P. Barros. Optimal Damping Between Two Adjacent Elastic Structures. *Earthquake Engineering and Structural Dynamics*, vol. 27, pp. 649-659, 1998.
[13] Y. L. Xu, Q. He and J. M. Ko. Dynamic response of damper-connected adjacent buildings under earthquake excitation. *Engineering Structures*, vol. 21, pp. 135-148, 1999.
[14] M. Abdullah, J. H. Hanif, A. Richardson and J. Sobanjo. Use of a shared tuned mass damper (STMD) to reduce vibration and pounding in adjacent structures. *Earthquake Engineering and Structural Dynamics*, vol. 30, pp. 1185-1201, 2001.
[15] R. E. Christenson, B. F. Spencer Jr., E. A. Johnson and K. Seto. Coupled Building Control Considering the effects of Building/Connector Configuration. *Journal of Structural Engineering*, ASCE, vol. 132, n. 6, pp. 853-863, 2006.
[16] L. A. Pérez, S. Avila and G. Doz. Seismic Response Control of Adjacent Buildings Connected by Viscous and Hybrid Dampers. *Dynamics of Civil Structures*, vol. 4, pp. 433-440, 2014.
[17] C. C. Patel. Seismic analysis of parallel structures coupled by lead extrusion dampers. *International Journal of Advanced Structural Engineering* (IJASE), vol. 9, pp. 177-190, 2017.
[18] A. S. Pippi. Resposta dinâmica para diferentes modelos de edificações adjacentes acopladas. Dissertação de Mestrado, Universidade de Brasília, Brasília, 2018.
[19] A. Pippi, P. Bernardes Júnior, S. Avila, M. de Morais, G. Doz. Dynamic Response to Different Models of Adjacent Coupled Buildings. *Journal of Vibration Engineering & Technologies*. Online publication. 2019
[20] N. R. Fisco and H. Adeli. Smart structures: Part II — Hybrid control systems and control strategies. *Scientia Iranica, Transaction A: Civil Engineering*, vol. 18, n. 3, pp. 275-284, 2011.
[21] A. H. Heidari, S.Etedali and M. R. Javaheri-Tafti. A hybrid LQR-PID control design for seismic control of buildings equipped with ATMD. *Frontiers of Structural and Civil Engineering*, Vol. 12, pp. 44-47, 2018.
[22] R. E. Klein and M. D. Healy, 1987. Semi-Active Control of Wind Induced Oscillations in Structures. *Proc. 2nd International Conference on Structural Control*, pp. 354-369.
[23] R. E. Christenson. Semiactive Control of Civil Structures for Natural Hazard Mitigation: Analytical and Experimental Studies. PhD Thesis, University of Notre Dame, 2001.
[24] H. Zhu, Y. Wen and H. Iemura. A Study on Interaction Control for Seismic Response of Parallel Structures. *Computers and Structures*, vol. 79, pp. 231-242, 2001.

[25] K. Bigdeli, W. Hare, J. Nutini and S. Tesfamariam. Optimizing damper connectors for adjacent buildings. *Optimization and Engineering*, vol. 17, pp. 47-75, 2016.
[26] F. Palacios-Quiñonero, J. Rubió-Massegú, J. M. Rossell and H. R. Karim. Integrated Design of Hybrid Interstory-Interbuilding Multi-Actuation Schemes for Vibration Control of Adjacent Buildings under Seismic Excitations. *Applied Sciences*, vol. 7, pp. 323-345, 2017.
[27] L. A. Pérez, S. Avila and G. Doz, 2015. Coupled structural dynamic response using passive dampers. *Proceedings of the XVII International Symposium on Dynamic Problems of Mechanics (DINAME)*.
[28] F. Palacios-Quiñonero, J. M. Rossell, J. Rodellar and H. R. Kamiri, 2011. Active-Passive Control Strategy for Adjacent Buildings. *American Control Conference*, pp. 3110-3115.
[29] K. S. Park, S. Y. Ok. Hybrid control approach for seismic coupling of two similar adjacent structures. Journal of Sound and Vibration, vol. 349, pp. 1-17, 2015.
[30] L. A. Pérez, S. Avila and G. Doz. Experimental study of the seismic response of coupled buildings models. *Procedia Engineering*, vol. 199, pp. 1767-1772, 2017.
[31] L. A. Pérez. Resposta Dinâmica de Edificações Adjacentes Acopladas: Considerações sobre a Interação Solo–Estrutura. Tese de Doutorado, Universidade de Brasília, 2017.
[32] S. Y. Chu, S. W. Yeh, L. Y. Lu and C. H. Peng. Experimental verification of leverage-type stiffness-controllable tuned mass damper using direct output feedback LQR control with time-delay compensation. *Earthquakes and Structures*, vol. 12, n. 4, pp. 425-436, 2017.
[33] C. M. Chang, S. Shia and C. Y. Chen. Design of Buildings with Seismic Isolation Using Linear Quadratic Algorithm. *Procedia Engineering*, vol. 199, pp. 1610-1615, 2017.
[34] S. Edetali and S. Tavakoli. PD/PID Controller Design for Seismic Control of High-Rise Buildings Using Multi-Objective Optimization: A Comparative Study with LQR Controller. *Journal of Earthquake and Tsunami*, vol. 11, n. 1, 2017.
[35] S. Bhattacharyya A. D. Ghosh and B. Basu. Design of an active compliant liquid column damper by LQR and wavelet linear quadratic regulator control strategies. *Structural Control and Health Monitoring*, vol. 25, n. 12, 2018.
[36] K. Miyamoto, D. Sato and J. She. A new performance index of LQR for combination of passive base isolation and active structural control. *Engineering Structures*, Vol. 157, pp. 280-299, 2018.
[37] K. Miyamoto, J. She, D. Sato and N. Yasuo. Automatic determination of LQR weighting matrices for active structural control. *Engineering Structures*, vol. 174, pp. 308-321, 2018.
[38] J. Kennedy and R. Eberhart, 1995. Particle swarm optimization. *Proceedings of IEEE International Conference on Neural Networks*, pp. 1942–1948.
[39] F. Shabbir. Particle Swarm Optimization with Sequential Niche Technique for Dynamic Finite Element Model Updating. *Computer-Aided Civil and Infrastructure Engineering*, vol. 00, pp. 1-17, 2014.